Theory and Practice of Science and Technology
2025, VOL. 6, NO. 10, 96-99
DOI: 10.47297/taposatWSP2633-456919.20250610

# GLCM-Based Correlation Analysis of Surface Topography and Perceived Color in Decorative Materials

Junhua Zhang[1]*, Yulin Zhu[2]

[1]Tsung-Dao Lee Institute, Shanghai Jiao Tong University, Shanghai, 201210, China

[2]Department of High School, Shanghai Starriver Bilingual School, Shanghai, 201108, China

**ABSTRACT**
This study how PP surface topography shapes color appearance. Light-blue and dark-blue samples were polished with SiC papers of varied grits to tune roughness. Optical micrographs were processed to compute GLCM features—ASM, contrast, sum average, sum variance, correlation, and entropy—describing microtexture. CIELAB L*, a*, b* values were measured and linked to texture. Spearman correlations show higher ASM and lower entropy—smoother morphology—associate with higher L* and greener–yellower hues. Canonical correlation analysis reveals a strong multivariate coupling (first r>0.94): entropy dominates the texture side, while a* and b* comparably dominate the color side. It lays a foundation for corresponding machine-learning inspection..

**KEYWORDS**
Gray-level co-occurrence matrix; Surface topography; Texture analysis; CIE L*a*b* color space

## 1 Introduction

Decorative materials pervade daily life, and color strongly influence design choices and consumer preference [1-2]. The apparent color of a solid is set jointly by chemistry and microstructure; even at fixed pigment composition, changes in surface topography alter the angular distribution of scattered light and thus the perceived hue, lightness, and saturation [3-4]. Across common decorative systems [5-6], there are strong couplings between surface processing and color appearance. Therefore, quantifying the relationship between surface roughness and color metrics is essential for controlling product appearance through precise surface engineering.

Ab initio electromagnetic simulations of irregular topographies are costly and not sensitive for irregular structure on surface, and reconstructing such detail is impractical for routine appearance control [7]. Digital image processing provides an efficient and non-destructive means to characterize surface morphology, offering a bridge between visual perception and quantitative surface analysis. Additionally, the gray-level co-occurrence matrix (GLCM) is a robust tool for describing surface texture at different spatial scales. Moreover, previous studies motivate us to explore how the texture variables correlate with perceptual color parameters, especially for L*, a*, b*. Because this color space provides a perceptual representation of colors [8].

This work builds a statistical framework that maps GLCM-derived texture variables to measured CIELAB color space. Section 2 details materials, imaging, colorimetry, and GLCM processing. Sec. 3 and Sec. 4 presents the statistical correlations between the GLCM features and measured color data, and discusses the physical interpretation of the relationships between topographical variation and color appearance. Finally, Sec.5 summarizes this work.

## 2 Materials & Methods

### 2.1 Samples Data Acquisition and Processing

As a typical decorative material, polypropylene (PP) was chosen in this study due to its widespread use in consumer products and stable response to surface processing. Two sets of PP sheets, in light blue and dark blue, were prepared and cut into 7 square samples of approximately $5 \times 5\ cm^2$ each. Six samples from each group were polished using ISO-standard silicon carbide (SiC) sanding sheets with grit sizes 120, 240, 400, 600, 800, and 1200. Polishing was performed manually with water-dampened sanding sheets in a radial cross motion, applying consistent pressure and rubbing 20 times per direction, to ensure thorough abrasion. After polishing, the samples were rinsed with flowing water for 30 seconds to remove residues and then dried naturally before subsequent measurements.

Then, microscopic photo of samples were taken using a Nikon DXM1200F optical microscope (Nikon Corporation, Japan) in bright-field mode at 40× lens under similar optical conditions. Figure 1(a) and 1(b) present the microscopic images of both sample sets. In addition, the colorimetric measurements were carried out using a PRECISION COLORIMETER NR10QC (Shenzhen ThreeNH Technology Co., Ltd., Guangdong, China) equipped with a 4 mm-diameter

* **Corresponding Author:** Junhua Zhang, 422671733@qq.com

circular aperture, providing color space in the CIELAB color space. For each sample, 20 independent measurements were taken to ensure statistical reliability (see Fig.1 (c) and (d)).

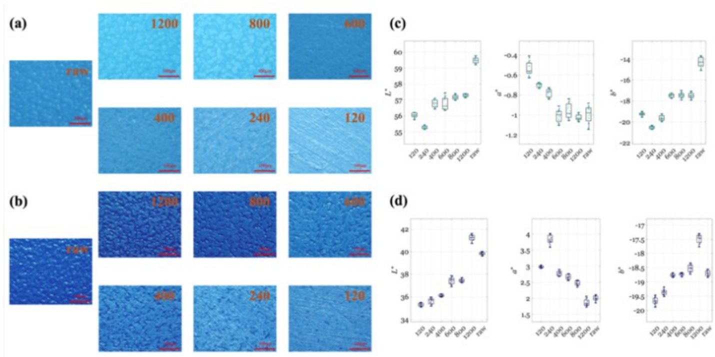


Figure 1 Microscopy of (a) light-blue and (b) dark-blue PP samples after polishing with 120–1200-grit papers and in the unpolished ("raw") state. The color measurements for the (c)light-blue and (d)dark-blue sets, respectively: 20 independent readings per sample shown as box plots

## 2.2 GLCM and its Feature Extraction

For a given offset distance d and orientation θ, the GLCM element P (i, j|d, θ) denotes the joint probability that a pixel with gray level i occurs adjacent to a pixel with gray level j at the specified relative position, which is:

$$P\left(i,j|d,\theta\right)=\frac{1}{N}\sum_{x=1}^{M}\sum_{y=1}^{N}\begin{cases}1, if I\left(x,y\right)=i \text{ and } I\left(x+\Delta x, y+\Delta y\right)=j\\ 0, \text{ otherwise}\end{cases} \quad (1)$$

where I(x, y) is the gray level at position (x, y), and(Δx, Δy) corresponds to the spatial offset defined by the d and θ. In practice, the GLCM generates numerous statistical features, but some of them effectively captures the essential characteristics of surface texture. Based on previous studies on strong-texture surface analysis [9], this study selects 6 features: Angular Second Moment (ASM, $\sum_i\sum_j P\left(i,j\right)^2$), Contrast ($\sum_i\sum_j\left(i-j\right)^2 P\left(i,j\right)$), Sum Average ($\sum_{k=2}^{2l} k\sum_i^l\sum_j^l P\left(i,j\right)$), Sum Variance ($\sum_{k=2}^{2l}\left(k-\text{SumAverage}\right)^2\sum_i^l\sum_j^l P\left(i,j\right)$), Correlation ($\sum_i\sum_j\left(i-\mu_i\right)\left(j-\mu_j\right)P\left(i,j\right)/\sigma_i\sigma_j$), and Entropy $-\sum_i\sum_j P\left(i,j\right)\log_2 P\left(i,j\right)$), where l is the number of gray levels (here l = 256), and $\mu_i$, $\mu_j$, $\sigma_i$, $\sigma_j$ denote the mean and standard deviation of gray-level indices. They collectively quantify texture smoothness, local roughness intensity, brightness distribution, texture strength, gray-level dependence, and randomness of the surface.

The original photos in Figure 1(a) and (b) were converted into 256-level grayscale images, smoothed using a local 5 × 5 mean filter to reduce noise. Each original image (1280 × 1024 pixels) was thereby divided into 20 subimages (256×256 pixels, see Figure 2(a)) to correspond with the number of color measurements. For each sub-image, GLCMs were calculated with of d = 8 and four orientations θ = [ 0◦, 45◦, 90◦, 135◦]; the results were averaged over all directions to eliminate orientation dependence (Figure 2(b)). The offset distance d = 8 was chosen as an optimal compromise from Ref. [10]. Subsequently, the six texture features were computed from the averaged GLCM for each sub-region (see Figure 2(c) for dark sample set).

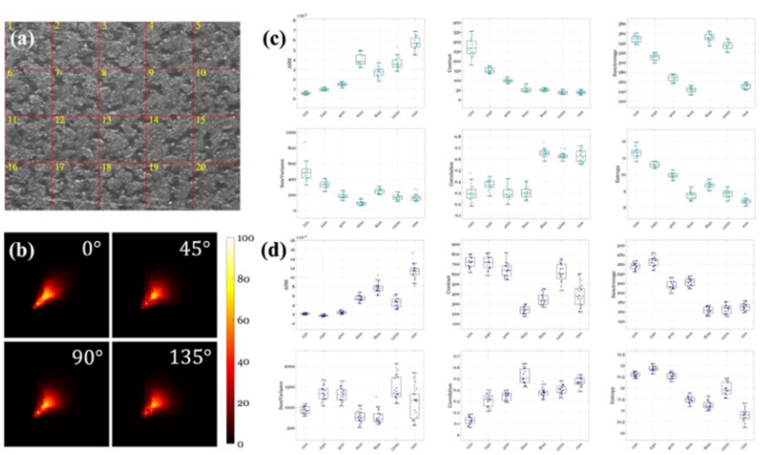


Figure 2 (a) Filtered grayscale image of the dark-blue sample polished with 400-grit sanding sheet, divided into 20 numbered sub-regions for texture analysis. (b) GLCM heat maps of the 8th sub-region from (a) at 4 θ orientations. Box plots showing the distributions of 6 GLCM-derived for all subregions of the (c) light sample set and (d) dark sample set

## 3 Correlation Between Surface Texture And Color Parameters

Figure 3 illustrates the Spearman's rank correlation coefficient matrices and presents the corresponding significance levels for all samples. Overall, both sample groups exhibit a highly consistent correlation pattern: with the exception of SumVariance, the remaining five texture features show similar relationships with the color components (L∗, a∗, b∗), and most Spearman coefficients are significant at the 0.95 confidence level.

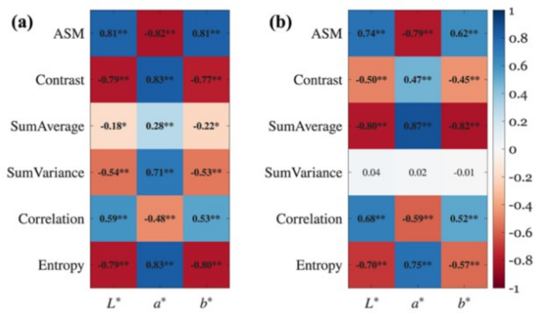


Figure3 Spearman's rank correlation coefficient matrices between GLCM texture features and L∗a∗b∗ color components for (a) light-blue and (b) dark-blue sample sets. Superscripts ** and * after each value respectively indicate their significance at $p < 0.01$and $p < 0.05$

ASM and entropy are dominant but opposite texture predictors for the same color channels. Higher ASM (lower entropy)—smoother, more uniform surfaces—yields higher L* and a yellow-green shift. Thus roughness modulates the specular/diffuse balance and chromaticity, consistent with Ref.[2] and Fig. 1. Correlation tracks ASM in both sets ($r \approx 0.5$), indicating no preferred orientation, as expected from radial-cross polishing.

Despite the general similarity, several distinctions can be identified. For light samples, contrast relates more strongly to all three color components, showing sensitivity to fine-scale intensity variations. For dark samples, SumAverage is more influential, highlighting the role of overall luminance under low reflectance; SumVariance is negligible, so large-scale gray-level changes contribute little.

## 4 Correlation Between Surface Texture and Color Parameters

In this section, canonical correlation analysis (CCA) was employed to evaluate the multivariate linear relationships between texture and color datasets, by identifying linear combinations of the two datasets that maximize their correlation. The GLCM features results were denoted as matrix X, while the L*a*b* color measurements were denoted as matrix Y. Before analysis, both X and Y were standardized by Z-score normalization to eliminate the effects of different measurement scales. Set A and B as the canonical coefficient matrices for X and Y, the canonical variables (or projections) matrices are U=XA and V=YB. Table. 1 summarizes the statistical tests for the light samples and dark samples. For both groups, the first pair of canonical variables exhibits the highest correlation ($r > 0.94$), indicating a strong linear relationship between GLCM-induced surface features and color measurements, consistent with the expected dominant contribution.

Table 1 CCA results for light and dark samples. The small Wilks' Λ indicate that the model explains most of the shared variance between the two datasets

| Sample Set | Pair No. of Canonical Variable | r | Wilks' Λ | p-value |
|---|---|---|---|---|
| Light | 1st | 0.9680 | 0.0168 | $1.02 \times 10^{-104}$ |
| | 2nd | 0.7916 | 0. 2669 | $9.48 \times 10^{-33}$ |
| | 3rd | 0.5340 | 0.7148 | $3.59 \times 10^{-9}$ |
| Dark | 1st | 0.9447 | 0.0199 | $6.11 \times 10^{-100}$ |
| | 2nd | 0.8651 | 0.1851 | $5.23 \times 10^{-43}$ |
| | 3rd | 0.5140 | 0.7358 | $2.38 \times 10^{-8}$ |

After such calculations, the first canonical variables $U_1$ (texture side) and $V_1$ (color side) for both two sample sets are expressed as:

$$U_{1,dark} = +1.551 \times ASM - 1.147 \times Contrast + 0.714 \times SumAverage + 0.092 \times SumVariance - 0.492 \times Correlation + 2.219 \times Entropy \quad (2a)$$

$$V_{1,dark} = -0.070 \times L^* + 0.562 \times a^* - 0.438 \times b^* \quad (2b)$$

$$U_{1,light} = +0.061 \times ASM - 0.695 \times Contrast + 0.127 \times SumAverage + 0.002 \times SumVariance - 0.398 \times Correlation + 1.379 \times Entropy \quad (2c)$$

$$V_{1,light} = -0.075 \times L^* + 0.479 \times a^* - 0.544 \times b^* \quad (2d)$$

Per Eq. 2(a – d), entropy has the largest positive loading in $U_1$, so textural irregularity dominates perceived color. Contrast carries a negative weight, meaning smoother textures reduce chromatic variation—an inverse link between uniformity and color modulation. Chromatically, a* and b* dominate while L* contributes little. With $a^* > 0$ and $b^* < 0$, higher entropy shifts hue toward the red – blue axis, indicating stronger chromatic modulation from microstructural complexity. Fig. 4 shows tight clustering and a strong linear trend; U1 orders surface treatments from raw to finely polished, yielding near-distinct clusters and a monotonic texture–color relation.

However, in dark samples, $U_1$ depends more on ASM and entropy, so fine-scale uniformity/randomness weigh more under low brightness. Light samples cluster differently: especially at intermediate polishing; dark samples form a tighter progression, indicating a more direct, consistent mapping.

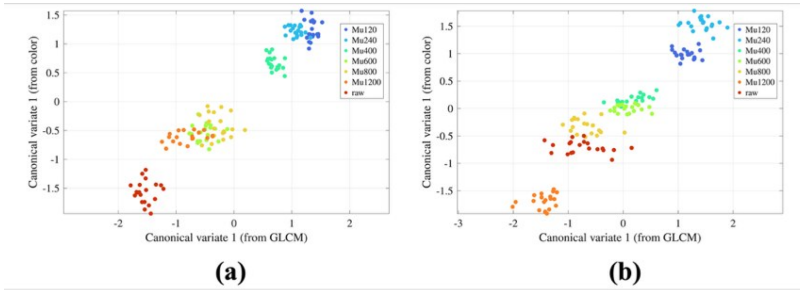


Figure 4 Scatter plots of the first canonical variates ($U_1$ vs. $V_1$) for (a) light and (b) dark sample sets. Each point denotes one measurement, each point color indicates one test sample

## 5 Conclusion

This study proposes a GLCM-based statistical correlation analysis method linking PP surface texture to perceived color. Spearman tests show consistent, significant ($p<0.05$) associations across light and dark PP: ASM and entropy display opposite, dominant relations with L*, a*, b*; higher ASM/lower entropy yield greater lightness and more green – yellow shifts. Sensitivity depends on base tone: contrast is most informative for light samples, SumAverage for dark; SumVariance contributes little, indicating macroscopic gray-level fluctuations weakly modulate color. Canonical correlation analysis further confirms this relationship: in the first canonical pair ($r>0.94$, $p<0.001$), Entropy carries the largest positive weight in $U_1$, whereas +a* and − b* dominate $V_1$, evidencing hue shifts along the red – blue axis. The monotonic progression of canonical scores with polishing demonstrates the coherent and quantifiable co-evolution of texture and appearance. This transferable approach underpins data-driven modeling and enables machine-learning – assisted inspection and control from digital images, with extensibility to other irregular rough surfaces.

## Acknowledgements

The authors declare that they have no known competing financial interests or personal relationships that could have appeared to influence the work reported in this paper.

## References

[1] L. Wei, J. Zhang, X. Gao, and R. Su, Study on optical discoloration of a material surface and its optical mechanism, Optik 223, 165371 (2020).

[2] J. Zhang, Z. Xu, and R. Su, Investigating color dynamics in composite lumbers: a diffractive approach to surface topography, Eur. Phys. J. Plus 139, 870 (2024).

[3] P. Sanmartín, B. Silva, and B. Prieto, Effect of Surface Finish on Roughness, Color, and Gloss of Ornamental Granites, J. Mater. Civ. Eng. 23, 1239–1248 (2011).

[4] J. Zhang and R. Su, Chromaticity analysis of diffraction pattern of white light under the grating, Optik 208, 164553 (2020).

[5] S. G. Kandi, B. Panahi, and N. Zoghi, Impact of surface texture from fine to coarse on perceptual and instrumental gloss, Prog. Org. Coat. 171, 107028 (2022).

[6] A. U. Güler, E. Güler, A. Ç. Yücel, and E. Ertaş, Effects of polishing procedures on color stability of composite resins, J. Appl. Oral Sci. 17, 2 (2009).

[7] H. M. Whitney, M. Kolle, P. Andrew, L. Chittka, U. Steiner, and B. J. Glover, Floral Iridescence, Produced by Diffractive Optics, Acts as a Cue for Animal Pollinators, Science 323, 130–133 (2009).

[8] Commission Internationale de l'Eclairage (CIE), Colorimetry, 3rd Edition, CIE Publication 015:2004 (CIE Central Bureau, Vienna, 2004).

[9] J. Yin, H. Qi, H. Feng, and X. Du, A method for wood surface defect detection based on mixed texture features, J. Zhejiang A&F Univ. 28, 937–942 (2011).

[10] H. Wang, Research on the pattern recognition methods of wood surface texture based on GLCM, Master's thesis, Northeast Forestry University, Harbin, China (2007).